Performance Analysis of Cooperative NOMA System

Sabra Akhtar Siddiqui[1], Saif Ahmad[2], Mohd Javed Khan[3]
[1, 2, 3] Dept of ECE
[1, 2, 3] Integral University, Lucknow, U.P.

Abstract- *A technology that holds promises for fifth generation (5G) wireless communications is non-orthogonal multiple access (NOMA). The integration of NOMA with cooperative relaying has lately gained growing interest because users with good channel conditions can function as relays to improve the system performance by using successive interference cancellation (SIC).*

An analytical approach for assessing the performance of a cooperative relaying system based on NOMA is proposed in this research. The exact expression of the average achievable rate is derived after studying NOMA's performance over Rician fading channels. In addition, we also suggest a Gauss-Chebyshev integration-based approximation method to determine the feasible rate. The numerical results support the strong match between our derived analytical results and the Monte Carlo simulations.

Keywords- NOMA, 5G, SIC, Rician fading, cooperative relaying.

I. INTRODUCTION

It is highly expected that future 5G networks should achieve a 10-fold increase in connection density, i.e., 106 connections per square kilometers [1]. Non-orthogonal multiple access (NOMA) has been proposed as a promising candidate to realize such an aggressive 5G goal [2]–[5]. NOMA is fundamentally different from conventional orthogonal multiple access (OMA) schemes such as FDMA, TDMA, OFDMA, etc., since it allows multiple users to simultaneously transmit signals using the same time/frequency radio resources but different power levels [3]–[5]. The key advantage of NOMA is to explore the extra power domain to further increase the number of supportable users. Specifically, users are identified by their channel conditions, those with good channel conditions are called strong users and others are called weak users. For the sake of fairness, less power are allocated to strong users at the transmitter side. In this way, the transmitter sends the superposition of signals with different power levels and the receiver applies successive interference cancellation (SIC) to strong users to realize multi-user detection [5], [6]. Such non-orthogonal resource allocation enables NOMA to accommodate more users and makes it promising to address the 5G requirement of massive connectivity, with the cost of controllable increase of complexity in receiver design due to SIC [5].In NOMA systems, the use of SIC implies that strong users have prior information about the messages of other users, so essentially they are able to serve as cooperative relays. Moreover, cooperative relaying is able to significantly enhance the system performance of cellular networks [7]. Thus, combining cooperative relaying and NOMA is promising to improve the throughput of future 5G wireless networks, and has attracted increasing interests recently [8]. Specifically, a cooperative NOMA transmission scheme was proposed in [9], where strong users decode the signals that are intended to others and serve as relays to improve the performance of weak users. Another NOMA-based cooperative scheme was proposed in [10], where the performance of a NOMA-based decode-and-forward relaying system under Rayleigh fading channel was studied. However, most of existing NOMA schemes only consider the Rayleigh fading channel, which is suitable for rich scattering scenarios without line of sight (LOS), while little attention has been drawn to the more general Rician fading channel, which takes both LOS and non LOS (NLOS) into consideration. In some typical 5G application scenarios, such as massive machine-type communications (mMTC) and Internet of things (IoT), “users” may be low-cost sensors deployed in a small area, where both LOS and NLOS exist, which can be better modeled by the Rician fading channel. In this paper, we investigate the performance of the NOMA-based cooperative relaying transmission scheme in [10] under Rician fading channels1 Evaluating system performance under Rician fading channel is rather challenging as the probability density function of Rician distribution variables consists of Bessel function, which makes it difficult to calculate the average achievable rate through integration. In order to derive the exact expression of the achievable rate, we propose an analytical method using Taylor expansion of Bessel function and incomplete Gamma function. However, the complexity of the incomplete Gamma function makes it still difficult to get the exact values, so we further propose an approximation method using Gauss-Chebvshev Integration to simplify the calculation. Finally, simulations confirm that our analytical results match well with the Monte Carlo results.

Comparing with wired communication, the wireless network has been the practical communication method due to its convenience and flexibility in varies environments. In

conjunction with the development of the beyond fifth-generation (5G) and sixth-generation (6G) mobile communications, various kinds of Internet of Things (IoT) devices (e.g., smart phones, smart watches and other IoT sensors) are designed and produced. The number of these devices is predicted to keep increasing in the upcoming years. Therefore, connecting massive number of devices through wireless signals will become more important. The most critical challenge for wireless systems is to find practical solutions in performance and secrecy improvement, i.e., to achieve reliable transmission and keep the information safe while improving data rates as well as confidentiality.

To cope with the above challenge, in this dissertation, a cooperative network technology is focused on, and the modern technologies to the emerging wireless scenarios is applied. In this paper, we will review these advanced schemes.

In order to achieve enhanced spectrum efficiency of the wireless mobile network, non orthogonalmultiple access (NOMA) has received attention by the researchers focusing on wireless systems [40–42]. Notably, different devices can share the same time and frequency spectrum with cooperative power allocation adjustment. Through the use of successive interference cancellation(SIC), the devices with weak power conditions can decode its own information after removing those strong power condition [43, 44], which has been investigated as an extension of the network-assisted interference cancellation and suppression (NAICS) in 3GPP [45, 46].

This technique significantly improve the spectral efficiency and outperform traditional orthogonal multiple access (OMA) schemes under the limitation of frequency spectrum. In Fig. 1, we illustrate the difference between OMA and NOMA. The OMA technique contains orthogonal frequency division multiple access (OFDMA) or time division multiple access (TDMA). In OFDMA, multiple devices are allocated with orthogonal subcarriers contacted via the orthogonal frequency-division multiplexing (OFDM) technique. In TDMA, the devices divide the signal into different time slots in order to share the same frequency channel. The downlink scenario with NOMA scheme is demonstrated in Fig. 1.2(a), where two devices (i.e., U1 and U2) receive information from a single base station (BS) with the same transmission channel. The BS continuously sends the signal to U1 and U2 simultaneously, where the two different signals are non-orthogonally superposed. In the decoding process, U1 needs to decode the signal of U2 and run SIC process of U2 signal before decoding its own signal.

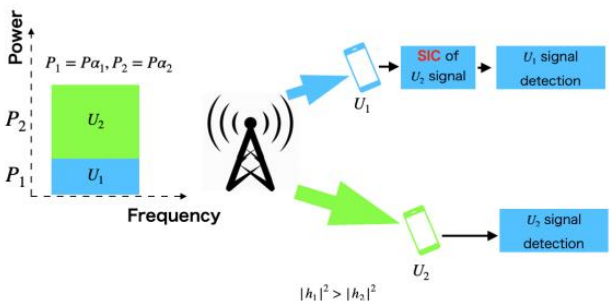

(a) NOMA

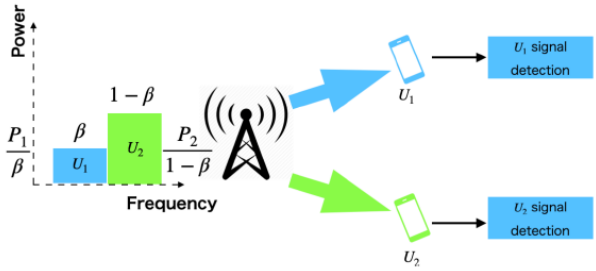

(b) OMA

Fig. 1: Multiple access scenarios for two devices that form a pair

II. SYSTEM MODEL

The system model of the NOMA-based cooperative relaying system is introduced in thispaper..We consider a simple cooperative relaying system (CRS) consisting of a source (S), decode-and-forward relay (R) which works in half-duplex mode, and a destination (D).We assume that all links between them (i.e., S-to-D, S to-R, and R-to-D) are available. The independent Rician fading channel coefficients of S-to-D, S-to-R, and R-to-D links are denoted as g_{SD} ,g_{SR}, and g_{RD} , with the average powers of ω_{SD} , ω_{SR} , and ω_{RD} , respectively. It is also assumed that $\omega_{SD} < \omega_{SR}$, since in general the path loss of the S-to-D link is usually worse than that of the S-to-R link [10]. In the traditional CRS presented in Fig. 2(a), the source transmits X_1 to the relay and destination in the first time slot. Then in the second time slot, the relay transmits X_2 to the destination. In this way, the destination only receives one signal in two time slots. In the NOMA-based CRS showed in Fig. 2(b), the destination is able to receive two different signals in two time slots, so it outperforms the traditional CRS in terms of throughput. Specifically, in the first time slot, the source transmits the superposition of two different data symbols s1 and s2 to the relay and the destination as follows:

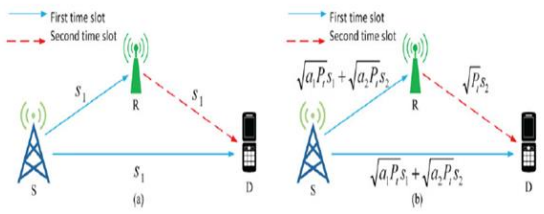

Fig. 2. System models of two cooperative relaying systems:

(a) Traditional cooperative relaying systems;
(b) NOMA-based cooperative relaying systems.

$$y = \sqrt{a_1 W_t} x_1 + \sqrt{a_2 W_t} x_2 \quad (1)$$

where x_i denotes the *i*-th data symbol with normalized power $E[|x_i|^2] = 1$, W_t is the total transmit power, and a_i is the power allocation coefficient. It is noted that $a_1 + a_2 = 1$, and $a_1 > a_2$ due to $\Omega_{SD}^2 < \Omega_{SR}^2$ [5]. Thus, the received signals r_{SR} and r_{SD} at the relay and the destination in the first time slot are respectively expressed as

$$r_{SR} = h_{SR}\left(\sqrt{a_1 W_t} x_1 + \sqrt{a_2 W_t} x_2\right) + n_{SR} \quad (2)$$

$$r_{SD} = h_{SD}\left(\sqrt{a_1 W_t} x_1 + \sqrt{a_2 W_t} x_2\right) + n_{SD} \quad (3)$$

where n_{SR} and n_{SD} denote the additive white Gaussian noise (AWGN) with zero mean and variance σ^2. The destination only decodes symbol x_1 by treating symbol x_2 as noise, while the relay acquires symbol x_2 from (1) using SIC. Thus, the received signal-to-interference plus noise ratios (SINRs) for symbols x_1 and x_2 at the relay can be respectively obtained as

$$\gamma_{SR}^1 = \frac{|h_{SR}|^2 a_1 W_t}{|h_{SR}|^2 a_1 W_t + \sigma^2} \quad (4)$$

$$\gamma_{SR}^2 = \frac{|h_{SR}|^2 a_2 W_t}{\sigma^2} \quad (5)$$

and the received SINR for symbol x_1 at the destination is obtained as

$$\gamma_{SD} = \frac{|h_{SD}|^2 a_1 W_t}{|h_{SD}|^2 a_1 W_t + \sigma^2} \quad (6)$$

perfectly decode symbol x_2 in the first time slot [5], the received signal at the destination in the second time slot can be expressed as

$$r_{RD} = h_{RD}\sqrt{W_t} x_2 + n_{RD} \quad (7)$$

where n_{RD} is the AWGN with zero mean and variance σ^2, and the received SINR for symbol x_2 in (7) can be obtained as

$$\gamma_{RD} = \frac{|h_{RD}|^2 W_t}{\sigma^2} \quad (8)$$

As the expressions for received signals and SINRs are already acquired, we will calculate both the exact and approximated achievable rates in the NOMA-based CRS in the next section.

In this paper, we first derive the exact expression of the average achievable rate of the NOMA-based CRS over Rician fading channel. As the exact value of achievable rates are difficult to calculate, we further propose an approximation method using Gauss-Chebyshev Integration to simplify the numerical calculation.

Achievable Rate Analysis :

In this subsection, we analyze the average achievable rate of x_1 and x_2. Let $\lambda_{SD} \triangleq |h_{SD}|^2$, $\lambda_{SR} \triangleq |h_{SR}|^2$, $\lambda_{RD} \triangleq |h_{RD}|^2$ and $\triangleq P_t/\sigma^2$, where ρ represents the transmit SNR. As both the relay and the destination must successfully decode x_1 and x_2, the rates of these two signals should be lower than the rates of both links calculated by Shannon formula, so the achievable rate is the minimum of the rates of two different links. According to [10], we can obtain the achievable rates C_{x_1} and C_{x_2} of signals x_1 and x_2 respectively as

$$C_{x_1} = \frac{1}{2} min\{log_2(1 + \gamma_{SD}), log_2(1 + \gamma_{SR}^1)\} = \frac{1}{2} log_2(1 + min\{\lambda_{SD}, \lambda_{SR}\}\rho - \frac{1}{2} log_2(1 + min\{\lambda_{SD}, \lambda_{SR}\}\rho a_2 \quad (9)$$

$$C_{x_2} = \frac{1}{2} min\{log_2(1 + \gamma_{SR}^2), log_2(1 + \gamma_{RD})\} = \frac{1}{2} log_2(1 + min\{a_2\lambda_{SR}, \lambda_{RD}\}\rho \quad (10)$$

Let $z_1 \triangleq min\{\lambda_{SD}, \lambda_{SR}\}$, $z_2 \triangleq min\{a_2\lambda_{SR}, \lambda_{RD}\}\rho$.According to [11],we can get the cumulative distribution function (CDF) of z_1 as

$$F(z_1) = 1 - A_x A_y \sum_{k=0}^{\infty}\sum_{n=0}^{\infty} \tilde{B}_x(n)\tilde{B}_y(k)\Gamma(n+1, a_x z_1)\times \Gamma(K+1, a_y z_1)$$

$$\overset{(a)}{=} 1 - A_x A_y \sum_{k=0}^{\infty}\sum_{n=0}^{\infty} \tilde{B}_x(n)\tilde{B}_y(k) n!\, k!\, e^{-(a_x+a_y)z_1} \times \sum_{i=0}^{n}\sum_{j=0}^{k} \frac{a_x^i a_y^j}{i!j!} z_1^{i+j} \quad (11)$$

Where $\tilde{B}_x(n) = (K_x^n (1+K_n)^n/(\Omega_x^n(n!))^2$, $\tilde{B}_y(K) = (K_x^n (1+K_n)^n/(\Omega_y^k(K!))^2$, $a_x = (1+K_x)/\Omega_x$, $a_y = (1+K_y)/\Omega_y$, $A_x = a_x e^{-kx}$, $A_y = a_y e^{-ky}$, $\tilde{B}_x(n) = B_x(n)/a_x^{n+1}$, $\tilde{B}_y(k) = B_y(k)/a_y^{k+1}$. The subscript x denotes the S-to-D link, y denotes the S-to-R link, w denotes the R-to-D link, and K is the Rician factor. Note that the expansion form of incomplete Gamma function is used for the second equality (a) of (11).Then, we prove the convergence of the infinite summation in (11) as follows:

Proof: Let $P_x = (K_x(1+K_x)/\Omega_x$, $Q_y = (K_y(1+K_y)/\Omega_y$, we have

$$\frac{\Gamma(n+1, a_x z_1)}{n!} < \frac{\Gamma(n+1)}{n!} < 1, \quad (12)$$

$$\frac{\Gamma(k+1, a_y z_1)}{n!} < \frac{\Gamma(n+1)}{n!} < 1 \ , (3.13)$$

Then

$$= A_x A_y \sum_{k=0}^{\infty}\sum_{n=0}^{\infty} \tilde{B}_x(n)\tilde{B}_y(k)\Gamma(n+1, a_x z_1)\times \Gamma(k+1, a_y z_1)$$

$$= A_x A_y \sum_{k=0}^{\infty}\sum_{n=0}^{\infty} \frac{P_x^n}{n!}\frac{Q_y^K}{k!}\frac{\Gamma(n+1, a_x z_1)}{n!}\frac{\Gamma(k+1, a_y z_1)}{k!}$$

$$< A_x A_y \sum_{k=0}^{\infty}\sum_{n=0}^{\infty} \frac{P_x^n}{n!}\frac{Q_y^K}{k!}$$

$$= A_x A_y e^{P_x+Q_y}$$

The final value will not change as k or n increases, so the infinite summation in (11) is convergent. Similarly, we can obtain the CDF of z_2 as follows:

$$G(z_2) = 1 - A_w A_y \sum_{n=0}^{\infty}\sum_{k=0}^{\infty} \tilde{B}_w(n)\tilde{B}_y(k)\Gamma(n+1, a_w z_2) \times \Gamma(K+1, \frac{a_y}{a_2} z_2)$$

$$= 1 - A_w A_y \sum_{k=0}^{\infty}\sum_{n=0}^{\infty} \tilde{B}_w(n)\tilde{B}_y(k) n!\, k!\, e^{-(a_w+\frac{a_y}{a_2})z_2} \times \sum_{i=0}^{n}\sum_{j=0}^{k} \frac{a_w^i(\frac{a_y}{a_2})^j}{i!j!} z_2^{i+j} \quad (14)$$

where the parameters in (14) are similarly defined as those in (11).After the CDF of $z_1 \triangleq min\{\lambda_{SD}, \lambda_{SR}\}$ has been obtained as (11),we can substitute it into (9), and then the average achievable rate $C_{x_1}$of the signal x_1 as shown in (9) can be expressed as

$$C_{x_1} = \frac{1}{2}\int_0^{\infty} [log_2(1+z_1\rho) - log_2(1+z_1\rho a_2)]dF(z_1)$$

$$= \frac{1}{2ln(2)}\left[\rho\int_0^{\infty}\frac{1-F(z_1)}{1+z_1\rho}dz_1 - \rho a_2\int_0^{\infty}\frac{1-F(z_1)}{1+z_1\rho a_2}dz_1\right] \quad (15)$$

Let $D(\rho) = \rho\int_0^{\infty}\frac{1-F(z_1)}{1+z_1\rho}dz_1$, and and substitute (11) into $D(\rho)$, we have

$$D(\rho) = \rho\int_0^{\infty}\frac{1-F(z_1)}{1+z_1\rho}dz_1$$

$$= A_x A_y \sum_{k=0}^{\infty}\sum_{n=0}^{\infty} \tilde{B}_x(n)\tilde{B}_y(k) n!\, k! \times \sum_{i=0}^{n}\sum_{j=0}^{k}\frac{a_x^i a_y^j}{i!j!} \int_0^{\infty}\frac{z_1^{i+j}e^{-(a_x+a_y)z_1}}{1+z_1\rho}d(z_1\rho)$$

$$\overset{(b)}{=} A_x A_y \sum_{k=0}^{\infty}\sum_{n=0}^{\infty} \tilde{B}_x(n)\tilde{B}_y(k) n!\, k! \times \sum_{i=0}^{n}\sum_{j=0}^{k}\frac{a_x^i a_y^j}{i!j!\rho^{i+j}} \int_0^{\infty}\frac{t^{i+j}e^{\frac{-(a_x+a_y)z_1}{\rho}}}{1+t}d(t) \quad (16)$$

Where (b) is obtained by setting $t = z_1\rho$

Now we have the following Lemma 1 to calculate the integral

$$\int_0^{\infty}\frac{t^{i+j}e^{\frac{-(a_x+a_y)z_1}{\rho}}}{1+t}d(t)$$ in (16)

Lemma 1: For $m \in \mathbb{Z}^*$ and $\beta > 0$, we have

$$\int_0^{\infty}\frac{t^m e^{-\beta t}}{1+t}d(t) = e^{\beta} m!\,\Gamma(-m, \beta), \quad (17)$$

Where
$\Gamma(-m,\beta) = \int_{\beta}^{\infty} \frac{e^{-t}}{t^{m+1}} dt$ denotes the incomplete Gamma function.

Proof: Let $x = \beta(1+t)$, we have

$$\int_0^{\infty} \frac{t^m e^{-\beta t}}{1+t} d(t) = \frac{e^{\beta}}{\beta^m} \int_{\beta}^{\infty} \frac{(x-\beta)^m e^{-x}}{x} dx \quad (18)$$

Then we define :

$$J_m(x) = \frac{(x-\beta)^m}{x}, \quad (19)$$

$$I(x) = \frac{e^{\beta}}{\beta^m} \int_{\beta}^{\infty} J_m(x)\, e^{-x} dx \quad (20)$$

On the one hand, by substituting (19) into (20), we have

$$I(x) = -\frac{e^{\beta}}{\beta^m} \int_{\beta}^{\infty} \frac{(x-\beta)^m e^{-x}}{x} d(e^{-x})$$

$$= -\frac{e^{\beta}}{\beta^m} \frac{(x-\beta)^m e^{-x}}{x}\Big|_{\beta}^{\infty} + \frac{e^{\beta}}{\beta^m} \int_{\beta}^{\infty} \frac{(x-\beta)^{m-1}(mx-x-\beta)}{x^2} e^{-x} d(x)$$

$$= \frac{e^{\beta}}{\beta^m} \int_{\beta}^{\infty} J_{m-1}(x)\, e^{-x} dx \quad (21)$$

We can observe from (21) that as long as β is a root of $J_m(x)$),the integral can be successively calculated by using (21) for m times. On the other hand, we know that $J_m(x) = \frac{(x-\beta)^m}{x} = x^{m-1} + a_{m-2}x^{m-2} + \ldots + a_0 + (-1)^m \beta^m / x$, so after m times of integration by part, we will have

$$I(x) = -\frac{e^{\beta}}{\beta^m} \int_{\beta}^{\infty} \frac{(x-\beta)^m e^{-x}}{x} d(e^{-x})$$

$$I(x) = -\frac{e^{\beta}}{\beta^m} \int_{\beta}^{\infty} \left(x^{m-1} + \ldots + a_0 + (-1)^m \frac{\beta^m}{x}\right)^{(m)} d(e^{-x})$$

$$I(x) = -\frac{e^{\beta}}{\beta^m} \int_{\beta}^{\infty} \left((-1)^m \frac{\beta^m}{x}\right)^{(m)} d(e^{-x})$$

$$= e^{\beta} m!\, \Gamma(-m,\beta), \quad (22)$$

where $(\cdot)^{(m)}$ denotes m-order derivation. Substitute (17) in Lemma 1 into (16), we can get the final exact expression of C_{x_1} as

$$C_{x_1} = \frac{1}{2\ln(2)} (D(\rho) - D(\rho a_2)), \quad (23)$$

Where

$$= A_x A_y \sum_{k=0}^{\infty} \sum_{n=0}^{\infty} \breve{B}_x(n) \breve{B}_y(k) n!\, k! \times \sum_{i=0}^{n} \sum_{j=0}^{k} \frac{(i+j)! a_x^i a_y^j}{i!\, j!\, \rho^{i+j}} e^{\frac{-(a_x+a_y)}{\rho}} \Gamma\left(-i-j, \frac{(a_x+a_y)}{\rho}\right), \quad (24)$$

and $D(\rho a_2)$ shares the same form as $D(\rho)$.Similarly, we can derive the exact expression of C_{x_2} as

$$C_{x_2} = \frac{1}{2\ln(2)} A_x A_y \sum_{k=0}^{\infty} \sum_{n=0}^{\infty} \breve{B}_x(n) \breve{B}_y(k) n!\, k! \times \sum_{i=0}^{n} \sum_{j=0}^{k} \frac{(i+j)! a_w^i (\frac{a_y}{a_2})^j}{i!\, j!\, \rho^{i+j}} e^{\frac{-\left(a_w+\frac{a_y}{a_2}\right)}{\rho}} \Gamma\left(-i-j, \frac{\left(a_w+\frac{a_y}{a_2}\right)}{\rho}\right), \quad (25)$$

Although we have derived the exact expressions of the achievable rates of x1 and x2 in (23) and (25) respectively, such expressions are very complicated, since the incomplete Gamma function is difficult to calculate. Thus, it is still difficult to get the exact values of the achievable rates, which motivates us to propose an approximation method to solve this problem in the next subsection.

Achievable Rate Approximation:

In this subsection, we propose an approximation method using Gauss-Chebyshev Integration [12] to simplify the numerical calculation of the incomplete Gamma function Γ(−m,β). However, Gauss-Chebyshev Integration is used on the limited interval [−1, 1], while the integral intervals in incomplete Gamma functions of (23) and (25) are infinite intervals. Thus, we set $t = 2\beta^{\frac{1}{x}} - 1$ and convert the incomplete Gamma function as

$$\Gamma(-m,\beta) = \left(\frac{1}{2\beta}\right)^m \int_{-1}^{1} \frac{1}{\sqrt{1-t^2}} (t+1)^{m-1} e^{\frac{-2\beta}{t+1}} \sqrt{1-t^2}\, dt$$

$$= \left(\frac{1}{2\beta}\right)^m \frac{\pi}{n} \sum_{i=1}^{n} \left(\cos\left(\frac{2i-1}{2n}\pi\right) + 1\right)^{m-1} \times e^{-\frac{2\beta}{\cos\left(\frac{2i-1}{2n}\pi\right)+1}} \left|\sin\left(\frac{2i-1}{2n}\pi\right)\right|, \quad (26)$$

where n is the approximation order. Substituting (26) into the exact expression of the achievable rate (23), we can finally obtain the approximation of (23) as

$$C_{x_1} = \frac{1}{2\ln(2)}\left(D(\rho) - D(\rho a_2)\right), \quad (27)$$

where

$$D(\rho) = A_x A_y \sum_{k=0}^{\infty}\sum_{n=0}^{\infty} \tilde{B}_x(n)\tilde{B}_y(k)\,n!\,k! \times \sum_{l=0}^{n}\sum_{j=0}^{k} \frac{(i+j)!\,a_x^l a_y^j}{i!\,j!\,\rho^{(i+j)}} \times e^{\frac{-(a_x+a_y)}{\rho}} \left(\frac{1}{2^{\frac{(a_x+a_y)}{\rho}}}\right)^{i+j} \frac{\pi}{n}\sum_{l=1}^{n}\left(\cos\left(\frac{2l-1}{2n}\pi\right)+1\right)^{i+j-1} \times e^{-\frac{2^{\frac{(a_x+a_y)}{\rho}}}{\cos\left(\frac{2l-1}{2n}\pi\right)+1}} \left|\sin\left(\frac{2l-1}{2n}\pi\right)\right|, \quad (28)$$

and $D(\rho a_2)$ shares the same form as $D(\rho)$.
Similarly, (25) can be approximated as

$$C_{x_2} = \frac{1}{2\ln(2)} A_x A_y \sum_{k=0}^{\infty}\sum_{n=0}^{\infty} \tilde{B}_x(n)\tilde{B}_y(k)\,n!\,k! \times \sum_{l=0}^{n}\sum_{j=0}^{k} \frac{(i+j)!\,a_w^l\left(\frac{a_y}{a_2}\right)^j}{i!\,j!\,\rho^{(i+j)}} \times e^{\frac{\left(a_x+\frac{a_y}{a_2}\right)}{\rho}} \left(\frac{1}{2^{\frac{\left(a_w+\frac{a_y}{a_2}\right)}{\rho}}}\right)^{i+j} \frac{\pi}{n}\sum_{l=1}^{n}\left(\cos\left(\frac{2l-1}{2n}\pi\right)+1\right)^{i+j-1} \times e^{-\frac{2^{\frac{\left(a_w+\frac{a_y}{a_2}\right)}{\rho}}}{\cos\left(\frac{2l-1}{2n}\pi\right)+1}} \left|\sin\left(\frac{2l-1}{2n}\pi\right)\right|, \quad (29)$$

Thus, the approximated achievable rates (27) and (29) can be conveniently calculated numerically, and their accuracy will be validated by the simulation results in the next paper.

III. RESULT

In this paper, we compare the analytical results obtained in the this paper with Monte Carlo simulations to validate their accuracy. Specifically, 10^5 realizations of Rician distribution random variables are generated, and the approximation order for Gauss-Chebyshev Integration is set as 100.

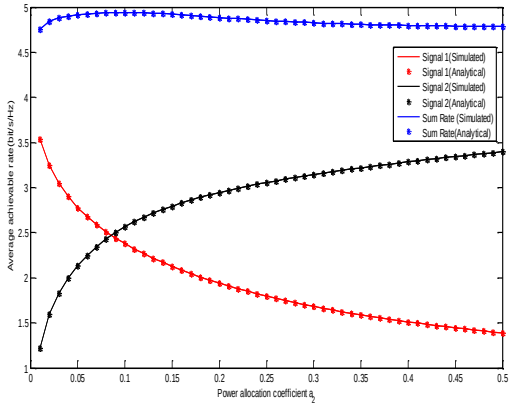

Fig.3. Achievable rates for the NOMA-based CRS over Rician fadingchannels.

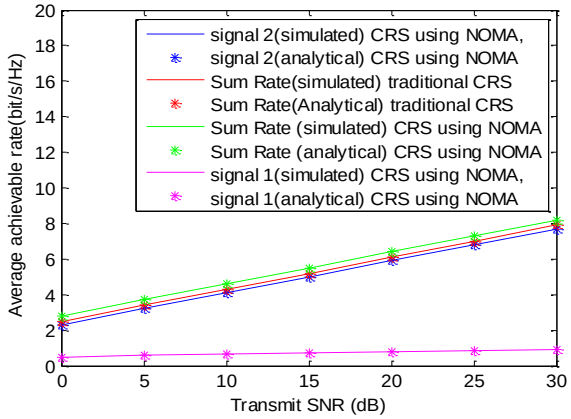

Fig. 4. Achievable rates comparison between the NOMA based CRS and traditional CRS

Fig. 3 presents the achievable rate performance of s1, s2 and the corresponding sum rate of the NOMA-based CRS against the power allocation coefficient a_2. In the model of Rician fading channel, the parameter Ω denotes the average power gain of the channel [13], which is usually determined by distances between transceivers. In our system , Ω_i ($i \in$ {SD, SR,RD}) denotes the average power gain of link SD, link SR, and link RD, mainly reflecting the impacts of distances

from S to D, from S to R, and from R to D, respectively. Thus, we set $\Omega_{SD} = 9 < \Omega_{SR} = \Omega_{RD} = 36$ [10], because the distances from S to R and from R to D are usually smaller than the distance from S to D, and thus link SR and link RD have higher average power gains than link SD. According to [11], other parameters are set as SNR = 20 dB, $K_{SR} = K_{RD} = 5$, and $K_{SD} = 2$. From Fig. 3, we can observe that the derived analytical results using Gauss-Chebyshev Integration match well with the simulation results. In addition, as a_2 increases, $s2$ will get more power and its achievable rate increases accordingly, while the achievable rate of $s1$

decreases. Moreover, the sum rate of two signals first increases and then slowly decreases with the increase of a_2. Actually, we can see from (10) that when a_2 is small, the achievable rate of s_2 is mainly determined by link SR, as $a_2\lambda_{SR}$ will always be smaller than λ_{RD} . Due to SIC, s_2 will have no interference in link SR, so increasing a_2 will largely increase the achievable rate of s_2, and thus increase the sum rate. However, when a_2 increases, $a_2\lambda_{SR}$ will be larger than λ_{RD} at last, and the rate of link RD will slowly become the determinant factor, which is not influenced by a_2.As a result, the increase of s_2 achievable rate finally cannot make up for the decrease of s_1's achievable rate, which causes the decrease of the sum rate, as shown in Fig. 3. Thus, there exists an optimal power allocation coefficient to maximize the sum rate, which is an interesting research topic deserving further investigation in the future. Fig. 4 compares the achievable rates of the traditional CRS and the NOMA-based CRS against the transmit SNR, where we set $a_2 = 0.4$,$\Omega_{SD} = 9$, $\Omega_{RD} = 36$, and $\Omega_{SR} = 144$. We find that the simulation results and analytical results are consistent, and the NOMA-based CRS achieves higher achievable sum rate than the traditional CRS, since NOMA-based CRS can transmit two signals in two slots, while traditional CRS can only transmit one signal during the same time.

V. CONCLUSION

In this paper, we have investigated the performance of a NOMA based cooperative relaying system by deriving the exact analytical expressions of the achievable rates. Moreover, an efficient approximation method using Gauss-Chebyshev Integration for the achievable rates was also proposed, which enables the sum series of the achievable rate expressions converge quickly. Simulation results have verified that our derived analytical results match well with the Monte Carlo simulations, and the NOMA-based CRS is able to achieve higher achievable rate than the traditional CRS.

REFERENCES

[1] K. J. R. Liu, A. K. Sadek,W. Su, and A. Kwasinski, Cooperative Communications and Networking. New York City, NY, USA: Cambridge University Press, 2009.

[2] P. N. Son and H. Y. Kong, "Cooperative communication with energy-harvesting relays under physical layer security," IET Commun., vol. 9, no. 17, pp. 2131–2139, Nov. 2015.

[3] R. Fan, J. Cui, S. Jin, K. Yang, and J. An, "Optimal node placement and resource allocation for UAV relaying network," IEEE Commun. Lett., vol. 22, no. 4, pp. 808–811, Apr. 2018.

[4] M. Ju and H.-C. Yang, "Optimum design of energy harvesting relay for two-way decode-and forward relay networks under max-min and max-sum criterions," IEEE Trans. Commun., vol. 67, no. 10, pp. 6682–6697, Oct. 2019.

[5] K. Sultan, "Best relay selection schemes for NOMA based cognitive relay networks in underlay spectrum sharing," IEEE Access, vol. 8, pp. 190 160–190 172, 2020.

[6] A. Sendonaris, E. Erkip, and B. Aazhang, "User cooperation diversity-part I: System description,"IEEE Trans. Commun., vol. 51, no. 11, pp. 1927–1938, Nov. 2003.

[7] "User cooperation diversity-part II: Implementation aspects and performance analysis," IEEE Trans. Commun., vol. 51, no. 11, pp. 1939–1948, Nov. 2003.

[8] R. U. Nabar, H. Bolcskei, and F. W. Kneubuhler, "Fading relay channels: Performance limits and space-time signal design," IEEE J. Sel. Areas Commun., vol. 22, no. 6, pp. 1099–1109, Aug. 2004.

[9] H. Cui, L. Song, and B. Jiao, "Multi-pair two-way amplify-and-forward relaying with very large number of relay antennas," IEEE Trans. Wireless Commun., vol. 13, no. 5, pp. 2636–2645, May 2014.

[10] S. Luo and K. C. Teh, "Amplify-and-forward based two-way relay arq system with relay combination,"IEEE Commun. Lett., vol. 19, no. 2, pp. 299–302, Feb. 2015.

[11] D. Li, "Amplify-and-forward relay sharing for both primary and cognitive users," IEEE Trans. Veh.Technol., vol. 65, no. 4, pp. 2796–2801, Apr. 2016.

[12] Y. Dong, M. J. Hossain, and J. Cheng, "Performance of wireless powered amplify and forward relaying over Nakagami-mfading channels with nonlinear energy harvester," IEEE Commun. Lett.,vol. 20, no. 4, pp. 672–675, Apr. 2016.

[13] S. Li, K. Yang, M. Zhou, J. Wu, L. Song, Y. Li, and H. Li, "Full-duplex amplify-and-forward relaying: Power and location optimization," IEEE Trans. Veh. Technol., vol. 66, no. 9, pp. 8458– 8468, Sep. 2017.

[14] K. M. Rabie and B. Adebisi, "Enhanced amplify-and-forward relaying in non-Gaussian PLC networks,"IEEE Access, vol. 5, pp. 4087–4094, 2017.

[15] L. Jiang and H. Jafarkhani, "mmWave amplify-and-forward MIMO relay networks with hybrid precoding/combining design," IEEE Trans. Wireless Commun., vol. 19, no. 2, pp. 1333–1346, Feb. 2020.

[16] A. S. Ibrahim, A. K. Sadek, W. Su, and K. J. R. Liu, "Cooperative communications with relay selection:When to cooperate and whom to cooperate with?" IEEE Trans. Wireless Commun., vol. 7, no. 7, pp. 2814–2827, Jul. 2008.

[17] M. R. Bhatnagar, R. K. Mallik, and O. Tirkkonen, "Performance evalution of best-path selection in a multihop decode-and-forward cooperative system," IEEE Trans. Veh. Technol., vol. 65, no. 4, pp.2722–2728, Apr. 2016.

[18] Y. Gu and S. Aissa, "RF-based energy harvesting in decode-and-forward relaying systems: Ergodic and outage capacities," IEEE Trans. Wireless Commun., vol. 14, no. 11, pp. 6425–6434, Nov. 2015.

[19] G. T. Djordjevic, K. Kansanen, and A. M. Cvetkovic, "Outage performance of decode-and-forward cooperative networks over Nakagami-m fading with node blockage," IEEE Trans. Wireless Commun.,vol. 15, no. 9, pp. 5848–5860, Sep. 2016.

[20] H. Liu, Z. Ding, K. J. Kim, K. S. Kwak, and H. V. Poor, "Decode-and-forward relaying for cooperative NOMA systems with direct links," IEEE Trans. Wireless Commun., vol. 17, no. 12, pp.8077–8093, Dec. 2018.

[21] R. Fan, S. Atapattu, W. Chen, Y. Zhang, and J. Evans, "Throughput maximization for multihop decode-and-forward relay network with wireless energy harvesting," IEEE Access, vol. 6, pp.24 582–24 595, 2018.

[22] O. M. Kandelusy and S. M. H. Andargoli, "Outage performance of decode-and-forward (DF)-based multiuser spectrum sharing relay system with direct link in the presence of primary users' power,"IET Commun., vol. 12, no. 3, pp. 246–254, Feb. 2018.

[23] E. Li, X. Wang, Z. Wu, S. Hao, and Y. Dong, "Outage analysis of decode-and-forward two-way relay selection with different coding and decoding schemes," IEEE Syst. J., vol. 13, no. 1, pp.125–136, Mar. 2019.

[24] M. Asadpour, B. Van den Bergh, D. Giustiniano, K. A. Hummel, S. Pollin, and B. Plattner, "Micro aerial vehicle networks: an experimental analysis of challenges and opportunities," IEEE Commun.Mag., vol. 52, no. 7, pp. 141–149, Jul. 2014.

[25] K. Namuduri, S. Chaumette, J. H. Kim, and J. P. G. Sterbenz, UAV Networks and Communications. Cambridge University Press, 2017.

[26] K. P. Valavanis and G. J. Vachtsevanos, Handbook of Unmanned Aerial Vehicles. Springer, 2015.

[27] F. Ono, H. Ochiai, and R. Miura, "A wireless relay network based on unmanned aircraft system with rate optimization," IEEE Trans. Wireless Commun., vol. 15, no. 11, pp. 7699–7708, Nov. 2016.

[28] M. M. Azari, F. Rosas, K.-C. Chen, and S. Pollin, "Ultra reliable UAV communication using altitude and cooperation diversity," IEEE Trans. Commun., vol. 66, no. 1, pp. 330–344, Jan. 2018.

[29] M. M. Azari, F. Rosas, and P. Sofie, "Cellular connectivity for UAVs: Network modeling, performance analysis, and design guidelines," IEEE Trans. Wireless Commun., vol. 18, no. 7, pp.3366–3381, Jul. 2019.

[30] W. Wang, X. Li, M. Zhang, K. Cumannan, D. W. K. Ng, G. Zhang, J. Tang, and O. A. Dober, "Energy-constrained UAV-assisted secure communications with position optimization and cooperative jamming," IEEE Trans. Commun., vol. 68, no. 7, pp. 4476–4489, Jul. 2020.

[31] H. Shakhatreh, A. H. Sawalmeh, A. Al-Fuqaha, Z. Dou, E. Almaita, I. Khalil, N. S. Othman,A. Khreishah, and M. Guizani, "Unmanned aerial vehicles (UAVs): A survey on civil applications and key research challenges," IEEE Access, vol. 7, pp. 48 572–48 634, 2019.

[32] W. Ejaz, M. A. Azam, S. Saadat, F. Iqbal, and A. Hanan, "Unmanned aerial vehicle enabled IoT platform for disaster management," Energies, vol. 12, no. 14, p. 2706, Jul. 2019.

[33] Y. Zeng, R. Zhang, and T. J. Lim, "Wireless communications with unmanned aerial vehicles: opportunities and challenges," IEEE Commun. Mag., vol. 54, no. 5, pp. 36–42, May 2016.

[34] J. Zhao, F. Gao, Q. Wu, S. Jin, Y. Wu, and W. Jia, "Beam tracking for UAV mounted Sat Com on the-move with massive antenna array," IEEE J. Sel. Areas Commun., vol. 36, no. 2, pp. 363–375,Feb. 2018.

[35] Y. Zeng, R. Zhang, and T. J. Lim, "Throughput maximization for UAV-enabled mobile relaying systems," IEEE Trans. Commun., vol. 64, no. 12, pp. 4983–4996, Dec. 2016.

[36] Y. Zhang, Z. Mou, F. Gao, L. Xing, J. Jiang, and Z. Han, "Hierarchical deep reinforcement learning for backscattering data collection with multiple UAVs," IEEE Internet Things J., vol. 8, no. 5, pp.3786–3800, Mar. 2021.

[37] J. Zhao, Y. Wang, Z. Fei, X. Wang, and Z. Miao, "NOMA-aided UAV data collection system: Trajectory optimization and communication design," IEEE Access, vol. 8, pp. 155 843–155 858,2020.

[38] F. Luo, C. Jiang, J. Du, J. Yuan, Y. Ren, S. Yu, and M. Guizani, "A distributed gateway selection algorithm for UAV networks," IEEE Trans. Emerg. Topics Comput., vol. 3, no. 1, Mar. 2015.

[39] R. Duan, J. Wang, C. Jiang, Y. Ren, and L. Hanzo, "The transmit-energy vs computation-delay trade-off in gateway-selection for heterogenous cloud aided multi-UAV systems," IEEE Trans.Commun., vol. 67, no. 4, pp. 3026–3039, Apr. 2019.

[40] M. Vaezi, R. Schober, Z. Ding, and H. V. Poor, "Non-orthogonal multiple access: Common myths and critical questions," IEEE Wireless Commun., vol. 26, no. 5, pp. 174–180, Oct. 2019.

[41] M. Vaezi and H. V. Poor, "NOMA: An information-theoretic perspective," in Multiple Access Techniques for

5G Wireless Networks and Beyond, M. Vaezi, Z. Ding, and H. V. Poor, Eds. Cham:Springer International Publishing, 2019, pp. 167–193.

[42] F. Mokhtari, M. R. Milli, F. Eslami, F. Ashtiani, B. Makki, M. Mirmohseni, M. Nasiri-Kenari, and T. Svensson, "Download elastic traffic rate optimization via NOMA protocols," IEEE Trans. Veh. Technol., vol. 68, no. 1, pp. 713–727, Jan. 2019.

[43] Z. Ding, M. Peng, and H. V. Poor, "Cooperative non-orthogonal multiple access in 5G systems,"IEEE Commun. Lett., vol. 19, no. 8, pp. 1462–1465, Aug. 2015.

[44] S. M. R. Islam, N. Avazov, O. A. Dobre, and K.-s. Kwak, "Power-domain non-orthogonal multiple access (NOMA) in 5G systems: Potentials and challenges," IEEE Commun. Surveys Tuts., vol. 19, no. 2, pp. 721–742, Second quarter 2017.

[45] 3GPP, "Study on network-assisted interference cancellation and suppression (NAICS) for LTE v.12.0.1," 3rd Generation Partnership Project (3GPP), Sophia Antipolis, France, Rep. TR 36.866, Mar. 2014.

[46] Media Tek, "Study on downlink multiuser superposition transmission (MUST) for LTE," 3rd Generation Partnership Project (3GPP), Hsinchu, Taiwan, Rep. TR 36.859, Apr. 2015.

[47] B. Wu, J. Chen, J. Wu, and M. Cardei, "A survey of attacks and countermeasures in mobile ad hoc networks," in Wireless Network Security, Y. Xiao, X. S. Shen, and D.-Z. Du, Eds. Boston, MA,USA: Springer, 2007, ch. 5, pp. 103–135.

[48] Y. Wang, G. Attebury, and B. Ramamurthy, "A survey of security issues in wireless sensor networks,"IEEE Commun. Surveys Tuts., vol. 8, no. 2, pp. 2–23, Second Quarter 2006.

[49] T. T. Karygiannis and L. Owens, "Wireless network security: 802.11, bluetooth and handheld devices," Gaithersburg, MD, USA, Nov. 2002.

[50] P. W. Shor, "Algorithms for quantum computation: discrete logarithms and factoring," in Proc.IEEE Annu. Symp. Found. of Comput. Sci. (FOCS), Santa Fe, NM, USA, Nov. 1994.

[51] R. K. Nichols and P. C. Lekkas, Wireless Security: Models, Threats, and Solutions. New York,NY, USA: McGraw-Hill, 2002.

[52] M. Bloch and J. Barros, Physical-Layer Security: From Information Theory to Security Engineering.Cambridge, United Kingdom: Cambridge University Press, 2011.

[53] A. D. Wyner, "The wire-tap channel," Bell Syst. Tech. J., vol. 54, no. 8, pp. 1355–1387, 1975.